Available online at www.sciencedirect.com
SCIENCE DIRECT
Catalysis Today 98 (2004) 43–54
CATALYSIS TODAY
www.elsevier.com/locate/cattod

Modeling in the development of hydrotreatment processes

G.F. Froment*

Department of Chemical Engineering, Texas A & M University, College Station, TX 77843-3122, USA

Abstract

The kinetic modeling of the hydrodesulfurization (HDS) process is based upon the detailed reaction network, distinguishes between the hydrogenolysis- and hydrogenation-steps and accounts for the adsorption of the various reacting species on two types of active sites. The functional form of the rate equations for the conversion of thiophene, (substituted) benzothiophene, (substituted) dibenzothiophene on Co/Mo-alumina appears to be identical. The nature of the active sites, the synergetic effect of Co-sulfides on the activity and the interconversion of sites by hydrogen and hydrogen sulfide are discussed. The application of rate equations accounting explicitly for the in situ conditioning of the catalyst and the HDS is illustrated for thiophene conversion. In the kinetic modeling of HDS of complex mixtures like light cycle oil, containing hundreds of S-components, the structural contribution approach is introduced to reduce the number of independent rate parameters. The structural contributions multiply the rate and adsorption parameters of the parent (unsubstituted) molecules and express the effect of the substituents. Their values were determined from experimental data. Commercial reactor operation for HDS of a complex mixture was simulated, including the effects of external and internal diffusion limitations. An example illustrates the gain that can be achieved in the removal of some of the most refractory S-components by intermediate flashing of H_2S.

Keywords: Hydrodesulfurization; Active sites; Kinetic modeling; Structural contributions; Simulation

1. Introduction

The legal restrictions on the sulfur-, nitrogen- and aromatics-content of petroleum fractions are getting more severe every year and have necessitated substantial adaptation of HDS- and HDN-processes, in particular also of the catalysts. The amount of work that has been devoted to Co–Mo or Ni–Mo on alumina catalysts is overwhelming. The majority of the published work deals with small-scale activity tests and catalyst characterization using the tools of solid-state chemistry and physics. Kinetic studies are often rudimentary and limited to single and simple components. The order is said to be one or, for mixtures, close to two. Clearly, if the conversion of S- and N-components has to get close to 100% to satisfy to day's legislation such simple rate laws do not permit an accurate ranking of catalyst, let alone a reliable design of reactors and their operation.

The present paper attempts to illustrate a more fundamental approach for the kinetic modeling of HDS accounting to a maximum extent for the information provided by the physico-chemical characterization. It considers detailed feedstock compositions but also transfer limitations and provides examples of application of an advanced reactor simulation model.

2. HDS reaction schemes

Figs. 1 and 2 show reaction schemes for the decomposition of 4-medibenzothiophene and of 4,6-dimedibenzothiophene [1]. For other substituted DBTs Fig. 1 is valid when the molecule is asymmetric, Fig. 2 when it is symmetric The figures show that the sulfur containing compound is converted along two parallel pathways. The first directly eliminates the S-atom by ''hydrogenolysis'', which is a scission of the C–S bond. The second starts with hydrogenation whose products subsequently undergo a C–S scission. There is now sufficient evidence that hydrogenolysis and hydrogenation steps occur on different sites, called σ for the first and τ for the second. The nature of these sites will be discussed in a later section. It is

* Tel.: +1 979 845 0406; fax: +1 979 845 6446.
E-mail address: g.froment@che.tamu.edu.

0920-5861/$ – see front matter © 2004 Elsevier B.V. All rights reserved.
doi:10.1016/j.cattod.2004.07.052

Nomenclature

a'_v	gas–liquid interfacial area per unit reactor volume (m_I^2/m_r^3)
a''_v	liquid–solid interfacial area per unit reactor volume (m_L^2/m_r^3)
$C_{Hs,Mo}$	spillover hydrogen concentration on Mo-sulfide phase (kmol/m^2)
C_i	molar concentration of component i (kmol/m^3)
C_{iG}	molar concentration of i in bulk of gas phase (kmol/m_G^3)
C_{iL}	molar concentration of i in bulk of liquid phase (kmol/m_L^3)
C_{iS}	molar concentration of i in fluid inside the solid (kmol/m_f^3)
C^i_{iS}	molar concentration of i in fluid at surface of solid (kmol/m_f^3)
C_{pG}	specific heat of gas phase (kJ/kg K)
C_{pL}	specific heat of liquid phase (kJ/kg K)
$C_{t,Mo}$	total molar concentration of potentially active and active sites on the molybdenum sulfide phase (kmol/m^2)
d_p	equivalent particle diameter (m_p)
d_r	reactor diameter (m_r)
D_{ie}	effective diffusivity of component i for transport in a pseudo-continuum (m_i^3/m_{cat} s)
f_G	friction factor
F_i	molar flow rate of component i (kmol/s)
h_f	heat transfer coefficient between liquid film and solid (kJ/m^2 s K)
h_G	heat transfer coefficient between gas and liquid (kJ/m^2 s K)
$(-\Delta H)$	heat of reaction (kJ/kmol)
H_i	Henry coefficient m_L^3/m_G^3, or partial molar enthalpy of species i (kJ/kmol)
H_{jv}	heat of vaporization of species i (kJ/kmol)
k	reaction rate coefficient (kmol/kg_{cat} s)
k_i	mass transfer coefficient from gas–liquid interface to liquid bulk, based on concentration driving force in liquid (m_L^3/m_I^2 s)
k_L	overall mass transfer coefficient from gas to liquid, based on concentration driving force in liquid (m_G^3/m_I^2 s)
K_A	adsorption equilibrium constant of component A (m^3/kmol)
$K_{i,\sigma}$	adsorption equilibrium constant of component i on σ-sites (Pa^{-1})
$K_{i,\tau}$	adsorption equilibrium constant of component i on τ-sites (Pa^{-1})
K_L	liquid–solid mass transfer coefficient (m_L^3/m_I^2 s)
$K_{\pi t}$	equilibrium constant of conversion of π-sites (Pa^b/(kmol/m^2 Mo)^a)
$K_{\sigma t}$	equilibrium constant of formation of σ-sites (Pa^d/(kmol/m^2 Mo)^c)
M	molecular mass of species i (kg/mol)
n	reaction order
N	number of species
N_i	rate of transfer of i from the gas bulk to the liquid bulk (kmol/m_i^2 s)
N_r	number of reactions
p_i	partial pressure of component i (Pa)
p_t	total pressure (Pa)
q	heat flux (kJ/m^2 s)
r_j	rate of reaction j (kmol/kg_{cat} s)
R	gas law constant (kJ/(kmol K))
Re_G	Reynolds number for the gas phase
Re_L	Reynolds number for the liquid phase
$s_{j,i}$	stoichiometric coefficient of component i in reaction j
S	matrix of stoichiometric coefficients
S_{Mo}	surface area of Mo-sulfide phase (m^2/(kmol Mo))
T	absolute temperature (K)
T_G, T_I, T_L, T_S	absolute temperature of gas, gas–liquid interface, liquid and solid, respectively
u_{sG}	superficial gas velocity (m_G^3/m_r^2 s)
u_{sL}	superficial liquid velocity (m_L^3/m_r^2 s)
x_i	mole fraction of component i in the liquid phase
y_i	mole fraction of component i in the gas phase
z	axial coordinate in reactor (m_r)

Greek symbols

β	Co- and Mo-sulfides content of catalyst (kmol/kg_{cat})
δ	two-phase frictional pressure drop, (Pa/m_r) also: highly sulfided, inactive sites
δ_G	frictional pressure drop per unit length, for gas flow only (Pa/m_r)
δ_L	frictional pressure drop per unit length, for liquid flow only (Pa/m_r)
ε	bed void fraction (m_f^3/m_r^3)
η	effectiveness factor of reaction
μ_g	gas viscosity (Pa s)
μ_L	liquid viscosity (Pa s)
ξ	radial coordinate inside particle (m_p)
π	potentially active sites
ρ	molar ratio Co/(Co + Mo) of catalyst
ρ_B	catalyst bulk density (kg_{cat}/m_r^3)
ρ_C	density of the catalyst (kg_{cat}/m_p^3)
ρ_G	gas density (kg/m_G^3)
ρ_L	liquid density (kg/m_L^3)
σ	hydrogenolysis site
τ	hydrogenation site

Ω	cross-section of reactor (m_r^2)
Subscripts	
f	fluid phase
G	gas phase
I	component *i*
I	interface
L	liquid phase
p	particle
t	total

evident also that dealing with the conversion of the feed component as a single reaction is an unsatisfactory approach for catalyst characterization and for the evaluation of its performance.

3. Rate equations

In writing rate equations for solid catalyzed processes based upon observable concentrations in the gas or fluid phase, the adsorption of the reactants and products have to be accounted for in an explicit way. It is clear that this excludes simple power law expressions, often found to be adequate in homogeneous reactions. Van Parijs and Froment [2,3] and Vanrysselberghe and Froment [4,5] extensively studied the kinetics of conversion of thiophene, benzothiophene, dibenzothiophene, 4-medibenzothiophene and 4,6-dimedibenzothiophene on one and the same Co–Mo/alumina catalyst. For each case all likely mechanisms were considered, thus leading to sets of rival kinetic models. Discrimination among these was based upon experimental data collected in a gas phase tubular reactor and in a multiphase Robinson–Mahoney reactor with complete mixing and was supported by physico-chemical tests on the parameters and statistical tests on both the parameter values and the rate equations. [6] For all the above mentioned compounds the rate equations turned out to have the same functional form as the one given here for dibenzothiophene (DBT) and leading to biphenyl (BPh), which is further converted into cyclohexylbenzene (CHB):

$$r_{\mathrm{DBT},\sigma} = \frac{k_{\mathrm{DBT},\sigma}K_{\mathrm{H},\sigma}K_{\mathrm{DBT},\sigma}C_{\mathrm{DBT}}C_{\mathrm{H_2}}}{\left(1 + K_{\mathrm{DBT},\sigma}C_{\mathrm{DBT}} + \sqrt{K_{\mathrm{H},\sigma}C_{\mathrm{H_2}}} + K_{\mathrm{BPh},\sigma}C_{\mathrm{BPh}} + K_{\mathrm{H_2S},\sigma}C_{\mathrm{H_2S}}\right)^3},$$

$$r_{\mathrm{DBT},\tau} = \frac{k_{\mathrm{DBT},\tau}K_{\mathrm{H},\tau}K_{\mathrm{DBT},\tau}C_{\mathrm{DBT}}C_{\mathrm{H_2}}}{\left(1 + K_{\mathrm{DBT},\tau}C_{\mathrm{DBT}} + \sqrt{K_{\mathrm{H},\tau}C_{\mathrm{H_2}}} + K_{\mathrm{BPh},\tau}C_{\mathrm{BPh}}\right)^3},$$

$$r_{\mathrm{BPh},\tau} = \frac{k_{\mathrm{BPh},\tau}K_{\mathrm{H},\tau}K_{\mathrm{BPh},\tau}C_{\mathrm{BPh}}C_{\mathrm{H_2}}}{\left(1 + K_{\mathrm{DBT},\tau}C_{\mathrm{DBT}} + \sqrt{K_{\mathrm{H},\tau}C_{\mathrm{H_2}}} + K_{\mathrm{BPh},\tau}C_{\mathrm{BPh}}\right)^3},$$

$$r_{\mathrm{CHB},\tau} = \frac{k_{\mathrm{CHB},\tau}K_{\mathrm{H},\tau}K_{\mathrm{CHB},\tau}C_{\mathrm{CHB}}C_{\mathrm{H_2}}}{\left(1 + K_{\mathrm{DBT},\tau}C_{\mathrm{DBT}} + \sqrt{K_{\mathrm{H},\tau}C_{\mathrm{H_2}}} + K_{\mathrm{BPh},\tau}C_{\mathrm{BPh}}\right)^3}. \quad (1)$$

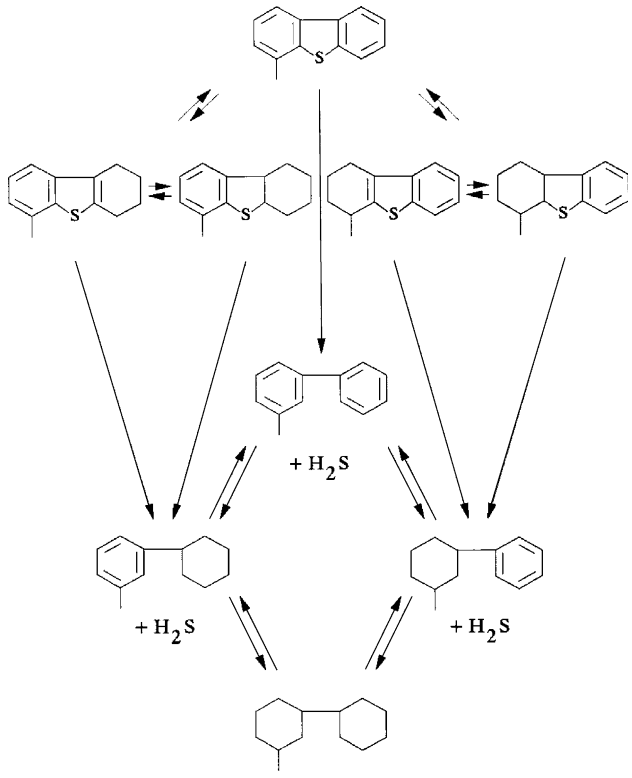

Fig. 1. HDS reaction scheme for 4-MeDBT. Reprinted with permission from Ref. [1], Copyright 1994, American Chemical Society.

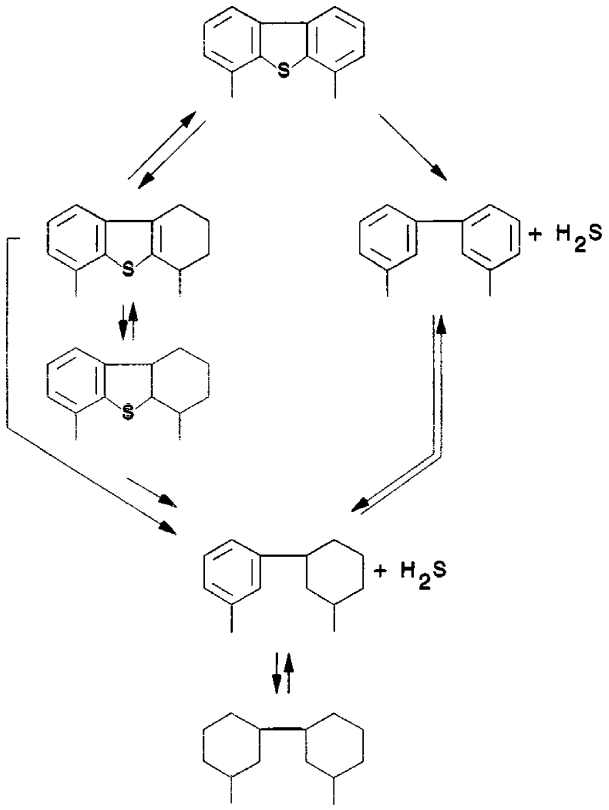

Fig. 2. HDS reaction scheme for 4,6-diMeDBT. Reprinted with permission from Ref. [1], Copyright 1994, American Chemical Society.

Table 1
Comparison of adsorption equilibrium constants and of the rate coefficients of hydrogenolysis and hydrogenation of these species

	$K_{i,\sigma}$	$K_{i,\tau}$	$k_{i,\sigma}$	$k_{i,\tau}$	
				$k^1_{i,\tau}$	$k^2_{i,\tau}$
DBT	75.6868	2.52021	1.58251×10^{-1}	3.08384×10^{-1}	
4-MeDBT	23.4677	2.61887	9.30744×10^{-2}	1.17834	6.86704×10^{-1}
4,6-DiMeDBT	18.0397	2.79914	1.34472×10^{-2}	2.05545	

These rate equations are intrinsic, i.e. they are free of mass transfer effects. The power 3 in the denominator reveals that three sites are involved in the rate determining step—which is the same for each case, namely the reaction between the adsorbed S-compound and hydrogen. The S-compound is adsorbed through its S-atom on one site, hydrogen competitively and dissociatively on two sites, thus leading to the square root of $K_H P_H$ in the denominator. Notice that the product H_2S is adsorbed on the σ-sites, but not on the τ-sites. For components appearing in both the hydrogenolysis and hydrogenation rate equations the adsorption equilibrium constants are found, based upon statistical tests, to be significantly different, which is in support of distinguishing between the sites required by those types of reaction. This is shown in Table 1 that compares adsorption equilibrium constants of DBT, 4-MeDBT and 4,6-diMeDBT on the σ- and τ-sites. Also shown are the rate coefficients, $k_{i,\sigma}$ and $k_{i,\tau}$, for the disappearance of these components according to the hydrogenolysis- and the hydrogenation-route. Table 2 compares the rates for typical conditions. For DBT the hydrogenolysis route is faster than the hydrogenation route, for 4-MeDBT they are roughly equal, but for 4,6-diMeDBT the hydrogenolysis rate is slower, because of steric hindrance of the two methyl-groups surrounding the S-atom through which the molecule is vertically adsorbed. Simulations based on these rate equations also show how the rates of hydrogenolysis of the three components drop with increasing H_2S concentrations in the liquid phase.

4. Active sites of the catalyst

Commercial HDS catalysts consist of Mo or W promoted by either Co or Ni and supported on alumina. The present paper focuses on CoMo/alumina catalysts. Such a catalyst is prepared by impregnation of the alumina support with solutions containing nitrates of Co and ammonium salts of Mo. After drying, calcination and removal of the decomposition products the catalyst consists of well dispersed but closely mixed MoO_2 and CoO on alumina. Sulfidation converts these oxides into MoS_2 and Co_9S_8. Under reaction conditions the sulfides tend to segregate, thus lowering the activity of the catalyst, however.

A hexagonal MoS_2 crystal has a layered structure. Single layers of Mo^{4+} are sandwiched between two layers of closely packed S^{2-} anions. Each Mo-atom is coordinated with six S-atoms and each S-atom with three Mo-atoms. To adsorb the S-containing reactants on the catalyst S-vacancies are required. These are created by hydrogen activation of the catalyst and yield Mo-atoms that are coordinatively unsaturated [7]. The energy required to remove S from the structure by means of hydrogen strongly varies with the number of Mo with which the S-atom is linked. At the corners and edges of the crystal coordinatively unsaturated Mo-atoms are more likely. To be really active, catalysts need in the first place small MoS_2 slabs. Fig. 3, which is a top view of a hexagonal MoS_2 crystal with $\bar{1}\,0\,1\,0$ and $1\,0\,\bar{1}\,0$ edges, illustrates that there are essentially three types of S–Mo links [8]. The S-atoms of the basal plane are linked to three Mo-atoms and removing them by means of hydrogen requires energy levels not available under HDS conditions. The removal of the bridging S-atoms is feasible, while that of the terminal S-atoms is easiest and leads to a more stable structure.

Table 2
Calculated rates of hydrogenolysis and hydrogenation in an equimolar ternary mixture of DBT, 4-MeDBT and 4,6-diMeDBT (0.017 kmol/m^3) at 673 K and a total pressure of 80 bar in the presence of hydrogen (0.257 kmol/m^3), H_2S (0.006 kmol/m^3) and biphenyl (0.031 kmol/m^3)

	$r_{i,\sigma}$ [kmol/kg$_{cat}$/h]	$r_{i,\tau}$ [kmol/kg$_{cat}$/h]	
		$r^1_{i,\tau}$	$r^2_{i,\tau}$
DBT	5.469×10^{-4}	2.486×10^{-5}	
4-MeDBT	9.973×10^{-5}	9.870×10^{-5}	5.752×10^{-5}
4,6-DiMeDBT	1.108×10^{-5}	1.840×10^{-4}	

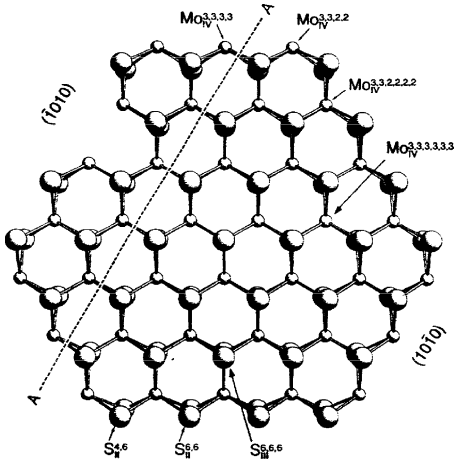

Fig. 3. MoS_2 slab. Reprinted with permission from Ref. [7] (Fig. 6.1, p. 220) Copyright 1996, Springer.

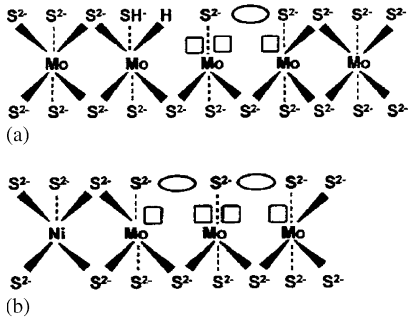

Fig. 4. (a) Hydrogenation center in CoMo-catalyst. (b) Hydrogenolysis center in CoMo-catalyst. Reprinted with permission from Ref. [10], Copyright 2000, Elsevier.

The singly bound S on the $1\,0\,\bar{1}\,0$ edge is less stable and will be removed more easily than the doubly bound S on the $\bar{1}\,0\,1\,0$ edge. Energy calculations show that molecular hydrogen is not efficient in the removal of S-atoms and that some type of atomic hydrogen is required for this, like the very reactive H-spillover species, emphasized by Delmon and co-workers [9] in the remote control model, to be discussed further in this paper.

Structures which are presently believed to be the active sites for respectively hydrogenation and hydrogenolysis are shown in Fig. 4a and b [10].

Hydrogenolysis- or σ-sites are more reduced than hydrogenation or τ-sites and can be formed out of these by further interaction with hydrogen. In other words: interconversion of sites under the action of hydrogen is possible [11]. Recent results of Kasztelan and co-workers [10] convincingly indicate that this interconversion is also possible by H_2S. It is clear that both hydrogen and the product H_2S condition the activity and selectivity of the catalyst and that the kinetic modeling of HDS should take this into account. The picture is not essentially different with Co- or Ni-promoted MoS_2.

The activity of MoS_2 for HDS greatly benefits from the addition of Co_9S_8 or from Ni-sulfides, although these compounds by themselves are only weakly active in HDS. The synergy between Mo and Co or Ni, illustrated in Fig. 5, [12] has led to lively scientific debates. According to the H. Topsoe group this synergy would result from the formation of a CoMoS phase that would be particularly active for HDS [13].

On the other hand it has been shown that this phase is not stable under HDS operating conditions. It may be that the decomposition of this phase leads to separate but very intimately mixed MoS_2 and Co_9S_8, a requirement for an active HDS catalyst. Delmon and co-workers have shown that mechanically prepared mixtures of both sulfides also show synergy [12]. This was ascribed to the formation on the Co-sulfide of a very active type of hydrogen, called spillover hydrogen, that would migrate to nearby MoS_2, efficiently create S-vacancies there and determine the ratio of τ- and σ-sites.[14] The ratio of hydrogenolysis to hydrogenation activity of the catalyst would thus be remotely controlled.

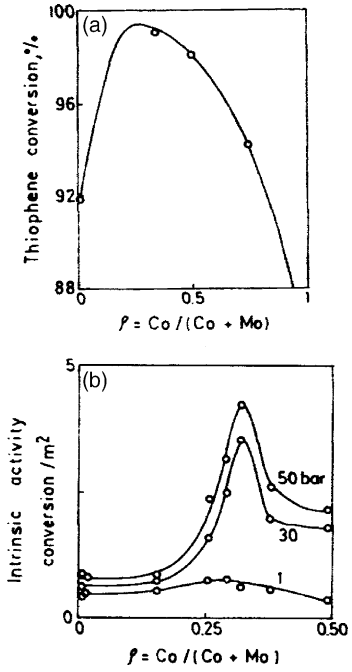

Fig. 5. (a) Effect of CoMo-ratio on the intrinsic activity of HDS on unsupported catalyst. (b) Effect of CoMo-ratio on the intrinsic activity of HDS on CoMo/alumina catalyst. Reprinted with permission from Ref. [15]. Copyright 1991, Elsevier.

5. Modeling catalyst conditioning and reaction in HDS

In a commercial HDS-reactor the catalyst is exposed to ratios of H_2 to H_2S which evolve with the axial distance and influence its composition, more particularly the number of σ- and τ-sites. These are determined by the conditioning of the catalyst, involving hydrogen activation and, during the actual operation, also by their interconversion, that depends upon the concentration of both hydrogen and the produced H_2S.

To account for this, Yu and Froment [15] explicited the total concentration $C^n_{\sigma,t}$ and $C^n_{\tau,t}$ of these sites in the rate Eq. (1) for hydrogenolysis and hydrogenation:

$$r_\sigma = k_\sigma C^n_{\sigma,\mathrm{t}}(\theta,\mathbf{P}) f_\sigma(\mathbf{K}_\sigma,\mathbf{P}),$$
$$r_\tau = k_\tau C^n_{\tau,\mathrm{t}}(\theta,\mathbf{P}) f_\tau(\mathbf{K}_\tau,\mathbf{P}). \quad (2)$$

θ is a vector of physical and kinetic constants pertaining to the mechanisms related to the role of spillover hydrogen, $\mathbf{K}_\sigma$ and $\mathbf{K}_\tau$ are vectors of adsorption equilibrium constants and $\mathbf{P}$ is a vector of partial pressures. The concentrations $C^n_{\sigma,t}$ and $C^n_{\tau,t}$ in (2) are generated by kinetic equations describing the rate of conditioning of the catalyst The combined process of finite-rate conditioning and HDS-reaction is schematically represented in Fig. 6.

For HDS of thiophene Yu and Froment derived the following rate equations for the hydrogenolysis of thiophene

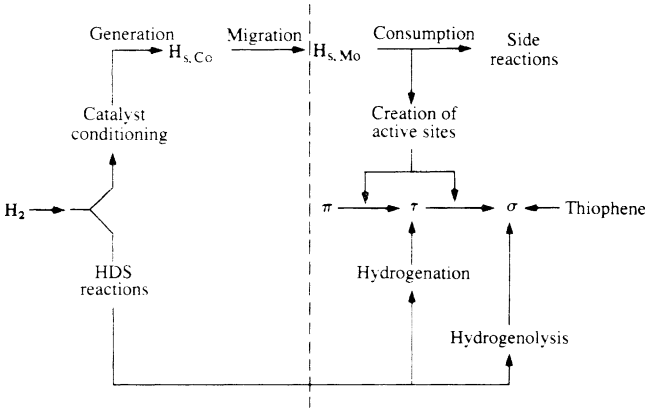

Fig. 6. Conditioning of catalyst, hydrogenolysis and hydrogenation. Reprinted with permission from Ref. [15]. Copyright 1991, Elsevier.

(T) and for the hydrogenation of the produced butenes (B) into butanes (A):

$$r'_\sigma = \left\{ \left[\frac{C_{t,Mo}((K_{\pi t}K_{\sigma t}C^{(a+c)}_{Hs,Mo})/(P_S^{(b+d)}))}{1 + ((K_{\pi t}C^{a}_{Hs,Mo})/P_S^{b}) + ((K_{\pi t}K_{\sigma t}C^{(a+c)}_{Hs,Mo})/(P_S^{(b+d)}))} \right]^2 \beta(1-\rho)S_{Mo} \right\} \times \frac{k_{T\sigma}K_{T\sigma}K_{H\sigma}P_T P_H}{(1 + K_{H\sigma}P_H + K_{T\sigma}P_T + K_{S\sigma}P_S/P_H)^2},$$

$$r'_\tau = \left\{ \left[\frac{C_{t,Mo}((K_{\pi t}C^{a}_{Hs,Mo})/P_S^{b})}{1 + ((K_{\pi t}C^{a}_{Hs,Mo})/P_S^{b}) + ((K_{\pi t}K_{\sigma t}C^{(a+c)}_{Hs,Mo})/(P_S^{(b+d)}))} \right]^2 \beta(1-\rho)S_{Mo} \right\} \times \frac{k_{B\tau}K_{B\tau}K_{H\tau}P_B P_H}{(1 + K_{H\tau}P_H + K_{A\tau}P_A + K_{B\tau}P_B)^2}. \quad (3)$$

Eq. (3) clearly reflect that the partial pressure of H_2S and, through the hydrogen spillover concentration, also the partial pressure of hydrogen, play a role not only in the HDS reactions but also in determining the catalyst composition. These steady state equations result from the combination of rate equations for the generation of spillover hydrogen on Co_9S_8, its migration over the alumina surface and the creation of active sites on MoS_2 and of rate equations for the HDS itself, with surface migration as rate determining step in the conditioning and the surface reaction between adsorbed species in the HDS. In these equations the factors inside the round brackets in r'_σ and r'_τ relate to the conditioning and represent respectively $C_{\sigma,t}$ and $C_{\tau,t}$ on the Mo-phase, in line with (2). The terms in the denominator result from the generation of spillover hydrogen (Hs), its migration and consumption. The powers a, b, c and d relate to the number of Hs involved in the various steps of the conditioning. The parameters in those equations were taken from the literature or derived from experimental data. Fig. 7a and b show the evolution of the rates of thiophene hydrogenolysis and the rates of hydrogenation of the produced butenes with the catalyst molar ratio, ρ, of Co/(Co + Mo) at various total pressures [15]. The curves are very similar to those of Fig. 5. The maxima for hydrogenolysis and hydrogenation do not occur at the same ratio of Co/(Co + Mo) although the unit molar surface areas of the Co- and Mo-sulfide phases were taken to be the same and independent of the catalyst composition. Measurements of the total surface area of the catalyst by Vrinat and de Mourgues [16] and Delvaux et al. [9] point towards a dependence of the Co- and Mo-phase surface areas upon ρ, with a maximum around $\rho = 0.3$. Introducing this into the model accentuates the maximum of the synergy curves and locates it in a different position. It also leads to a peak in the spillover hydrogen concentration on the Mo-sulfide versus ρ-curve, instead of a monotonically increasing value. Clearly, the model enables the effect of

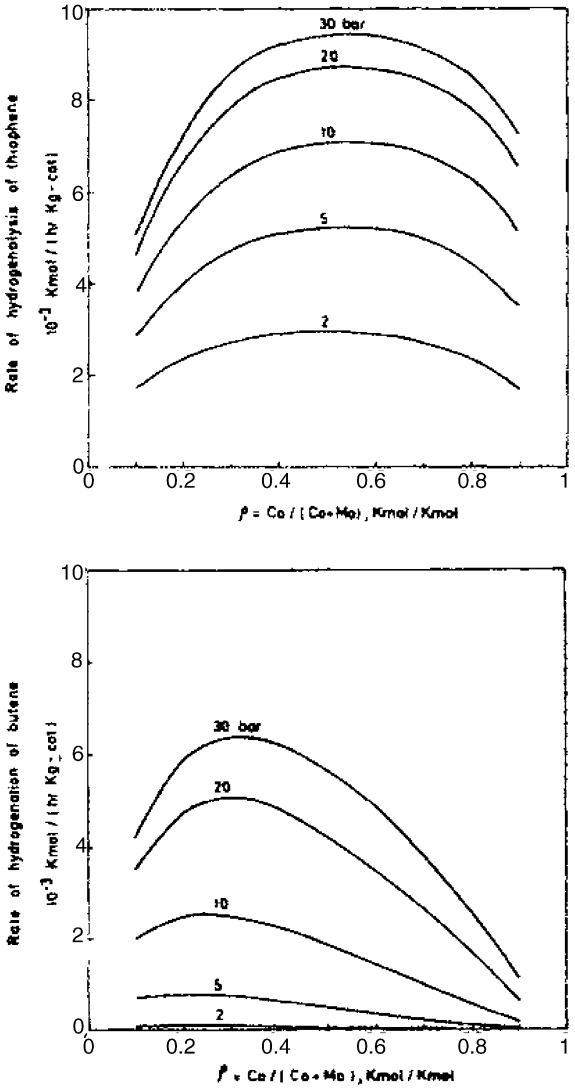

Fig. 7. (a) Rate of hydrogenolysis of thiophene at various total pressures vs. Co/Mo ratio. (b) Rate of hydrogenation of butenes at various total pressures vs. Co/Mo ratio. Reprinted with permission from Ref. [15]. Copyright 1991, Elsevier.

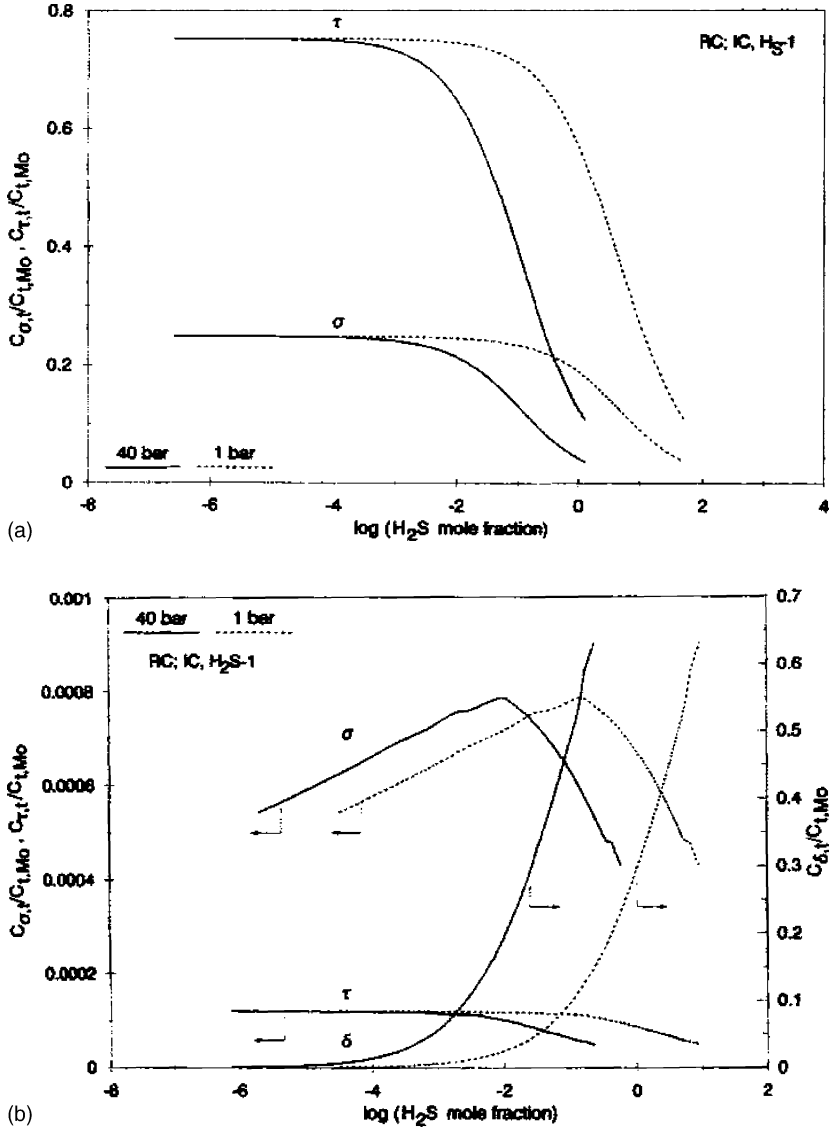

Fig. 8. (a) Evolution of relative σ- and τ-site concentration with H_2S mol fraction. Remote control model and interconversion of τ- and σ-sites by spillover hydrogen. (b) Evolution of relative σ- and τ-sites concentration with H_2S mol fraction. Remote control and interconversion of τ- and σ-sites by means of H_2S. Reprinted with permission from Ref. [19]. Copyright 1994, Elsevier.

catalyst properties to be investigated and quantified and thus provide interesting information for further catalyst development.

Relaxing the condition of a rate determining step Van Parijs and Froment [17] identified regions in the parameter space where multiple values for $H_{s,Mo}$ would be possible. Experimental results of Broderick et al. [18] on the effect of catalyst pretreatment on its activity may be interpreted in terms of the existence of multiple steady states.

Pille et al. [19] extended the approach of Yu and Froment [15] to a situation in which interconversion is caused by H_2S, as suggested by Kasztelan and co-workers [12]. Their experimental database for the HDS of thiophene was obtained in a continuous Berty reactor, operating with complete mixing and with partial pressures of H_2S ranging from 0.2 to 5.5 bar. The remote control models explicitly considering the finite-rate conditioning by Hs and the interconversion of sites by Hs or by H_2S turned out to be superior to a number of rival classical Hougen–Watson models with a fixed number of sites, even those containing a second type of σ-site resulting from the instantaneous effect of H_2S on S-vacancies. Fig. 8a and b show the results of simulations based upon the remote control model with interconversion respectively by Hs and by H_2S [19]. In the first case the concentrations of σ- and τ-sites on the MoS_2 monotonously decrease with increasing H_2S partial pressure, but in the second case a maximum is observed in the concentration of σ-sites. In the HDS-work reported in the literature the H_2S concentration is generally high and the experiments thus led to conditions on the downhill side of the curve. In HDN work the H_2S concentration is generally lower, leading to concentrations of σ-sites on the uphill side of the curve. Indeed, an increase of the HDN rate by H_2S additions is observed.

6. HDS of complex mixtures

The kinetics of the conversion of mixtures of S-containing components have generally been formulated in terms of a single S-lump and homogeneous type rate equations. An order between 1.5 and 2.0 is generally obtained. Such an approach, leading to rate coefficients which vary with the feedstock and even with the operating conditions, is definitely not the way to go. Instead, a distinction has to be made between the conversion of the components by hydrogenolysis and hydrogenation and the adsorption of the various species has to be accounted for, resulting in Hougen–Watson-type rate equations. Unfortunately, oil fractions contain a large number of S-components and dealing with these on an individual basis along conventional lines would lead to an overwhelming number of rate- and adsorption-parameters.

Consider the HDS of DBT and substituted DBT, e.g. 4-MeDBT and 4,6-DBT by hydrogenolysis and hydrogenation and the hydrogenation of biphenyl into the corresponding cyclohexylbenzene (viz Figs. 1 and 2).

In Section 3 it was mentioned that the rate equations for DBT and various substituted DBT were found to have the same functional form. There are 44 sDBT, therefore 44 adsorption equilibrium constants, $K_{(sDBT),\sigma}$, for these components on the σ-sites and 44 rate coefficients, k, for their hydrogenolysis producing 29 sBPh, yielding 29 $K_{(sBPh)}$. The adsorption of the feed hydrogen leads to one $K(H_2)$ and that of the product H_2S to one $K(H_2S)$. Accounting for the adsorption of the sDBT on the τ-sites requires another 44 parameters, $K_{(sDBT),\tau}$, and for their hydrogenation another 84k. The adsorbed sBPh lead to 29 $K_{(sBPh),\tau}$, the hydrogenation of the sBPh to 55k, the adsorption of H_2 to one $K(H_2)$. Adding two adsorption K and one rate coefficient k for the hydrogenolysis of DBT itself and $2K + 2k$ for the hydrogenation of DBT leads to a total of 339 rate parameters, as shown in Table 3. Clearly, their value cannot be determined significantly from any reasonable experimental program.

This led Froment et al. [1] to introduce the "structural contribution" approach in which the rate- and adsorption parameters of substituted components are related to those of the "parent" molecule by accounting for the electronic effect and steric hindrance exerted by the substituent(s).These have a number of common characteristics that permit a drastic reduction of the number of independent parameters.

6.1. Structural contributions

On σ-sites the S-containing components are vertically adsorbed through their S-atom so that in hydrogenolysis electronic and steric effects have to be considered separately. Methyl-groups beyond the α-position with respect to the S-atom only exert an electronic effect on the adsorption and reaction step. This effect is considered to depend only on the number of substituents, not on their position. Methyl-groups

Table 3
Number of parameters in kinetic model: HDS of DBT and sDBT

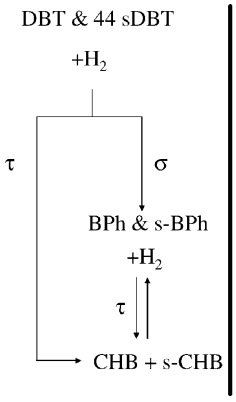

	Number of Parameters, Approach: Classical σ	Classical τ	Structural Contributions σ	Structural Contributions τ
$K_{(s)DBT}$	45	45	5+1	3+1
$k_{(s)DBT}$	45	85	5+1	3+1
$K_{(s)BPh}$	30	30	3+1	3+1
$k_{(s)BPh}$	-	56	-	2+1
K_{H2}	1	1	1	1
K_{H2S}	1	-	1	-
Total	339		34	

in 4 and 4,6 position, which are in α-positions with respect to the S-atom exert both electronic and steric hindrance effects on the rates.

Based upon these assumptions the equilibrium constant for the adsorption of the various substituted DBT on the σ-sites, $K_{sDBT,\sigma}(m;n;p)$, is related to that of the parent molecule, $K_{DBT,\sigma}$ through the following expression in which the structural contributions are written in italic:

$$K_{sDBT,\sigma}(m;n;p) = K_{DBT,\sigma} K_{EL,\sigma}^{sDBT}(m;n;p) K_{ST,\sigma}^{sDBT}(m;n;p). \quad (4)$$

m, n and p indicate the position of the Me-group in mono-, di-, and tri-substituted DBT. Only three structural contributions are required to account for the electronic effect of the substituents and two for the steric hindrance effect when there are substituents in α-position with respect to the S-atom. If there is one substituent in 4- or 6-position $K_{ST,\sigma}^{sDBT}(m;n;p)$ is written $K_{ST,\sigma}^{sDBT}(4;0;0) = (K_{ST,\sigma}^{sDBT}(6;0;0)$, given the symmetry with respect to the S-atom), when there are substituents in both 4- and 6-positions: $K_{ST,\sigma}^{sDBT}(4;6;p)$.

The same can be done for the rate coefficients of the hydrogenolysis reactions of the substituted DBT

$$k_{sDBT,\sigma}(m;n;p) = k_{DBT,\sigma} k_{EL,\sigma}^{sDBT}(m;n;p) k_{ST,\sigma}^{sDBT}(m;n;p). \quad (5)$$

Again only five structural contributions are required.

For the adsorption of species on τ-sites, which is considered to be flat, only the number of substituents and not their position has to be taken into account, so that the electronic and steric hindrance effects may be lumped. In this case only three structural contributions, describing the electronic and steric hindrance effects of one, two and three substituted DBT, are required:

$$K_{sDBT,\tau}(m;n;p) = K_{DBT,\tau} K_{EL+ST,\tau}^{sDBT}(m;n;p). \quad (6)$$

For the hydrogenation reactions between species adsorbed on the τ-sites:

$$k_{sDBT,\tau} = k_{DBT,\tau} k^{sDBT}_{EL+ST,\tau}(m;n;p), \quad (7)$$

and again only three structural contributions are required.

Table 3 shows that if only the disappearance of DBT and of the 44 sDBT through hydrogenolysis and hydrogenation were considered only 34 parameters would have to be determined: 24 structural contributions to rate coefficients and adsorption constants of sDBT and sBPh plus three rate coefficients related to DBT and BPh and seven constants accounting for the adsorption of DBT, BPh, H_2 and H_2S.

6.2. Application to hydrodesulfurization of light cycle oil (LCO)

Hougen–Watson type rate equations for the hydrogenolysis of DBT, 4-MeDBT and 4,6-diMeDBT were obtained by Vanrysselberghe and Froment [4] and Vanrysselberghe et al. [5] in a completely mixed continuous Robinson–Mahoney reactor for one and the same catalyst. Rigorous discrimination between rival models consistently led to the same form, shown below accounting for the structural contribution approach.

$$R_{sDBT} = C_{sDBT} C_{H_2} \left[\frac{f_{sDBT,\sigma} k_{DBT,\sigma} K_{DBT,\sigma} K_{H,\sigma}}{DEN_\sigma} + \frac{f_{sDBT,\tau} k_{DBT,\tau} K_{DBT,\tau} K_{H,\tau}}{DEN_\tau} \right], \quad (8)$$

with

$$DEN_\sigma = \left(1 + \sum_i K_{i,\sigma} C_i + \sqrt{K_{H,\sigma} C_{H_2}}\right)^3,$$

$$DEN_\tau = \left(1 + \sum_i K_{i,\tau} C_i + \sqrt{K_{H,\tau} C_{H_2}}\right)^3. \quad (9)$$

$f_{sDBT,\sigma}$ is a multiplication factor for the term related to the σ-sites. For a triMeDBT with a Me group in 4 and one in 6-position it can be explicited as follows:

$$f_{sDBT,\sigma} = k^{sDBT}_{EL,\sigma}(m;n;p) K^{sDBT}_{EL,\sigma}(m;n;p) k^{sDBT}_{ST,\sigma}(4;6;0) \times K^{sDBT}_{ST,\sigma}(4;6;0). \quad (10)$$

$f_{sDBT,\tau}$ is related to the τ-sites and can be written:

$$f_{sDBT,\tau} = k^{sDBT}_{EL+ST,\tau}(m;n;p) K^{sDBT}_{EL+ST,\tau}(m;n;p). \quad (11)$$

The denominators of (8), represented in more detail in (9), contain the concentrations of all the adsorbing species, multiplied by their adsorption equilibrium constants. With a mixture like LCO not all components can be identified, so that only the total numerical value of DEN_σ and DEN_τ can be determined from the experiments. From rate measurements in the HDS of LCO the variation of DEN_σ and DEN_τ with composition and temperature can be obtained when the products $k_{i,\sigma}K_{i,\sigma}K_{H,\sigma}$ and $k_{i,\tau}K_{i,\tau}K_{H,\tau}$ that appear in the numerator and that do not depend upon the mixture composition are known from experiments with the parent molecule DBT. An example for LCO is given in Fig. 9 [20]. With a mixture like LCO the definition of conversion is a weighted and normalized average of the individual conversions of a number of selected components

$$\bar{x} = \frac{1}{\sum_{i=1}^{7} y_i} \sum_{i=1}^{7} x_i y_i. \quad (12)$$

For a given temperature the coverage of the τ-sites increases and that of the σ-sites decreases with the molar averaged conversion. The reacting species in the LCO mixture adsorb to a higher extent on the σ-sites than the reaction products. The adsorption decreases as the temperature increases and the values of DEN decrease [20].

The values of the structural contributions for the hydrogenolysis and hydrogenation of mono- and di-substituted DBT in the temperature range 513–593 K were obtained from data on HDS of LCO, 4-MeDBT and 4,6-diMeDBT [20]. By way of example Table 4 shows the set of values at 573 K.

Whereas substituents which are not in α-position do not exert electronic effects, neither on the adsorption on σ-sites

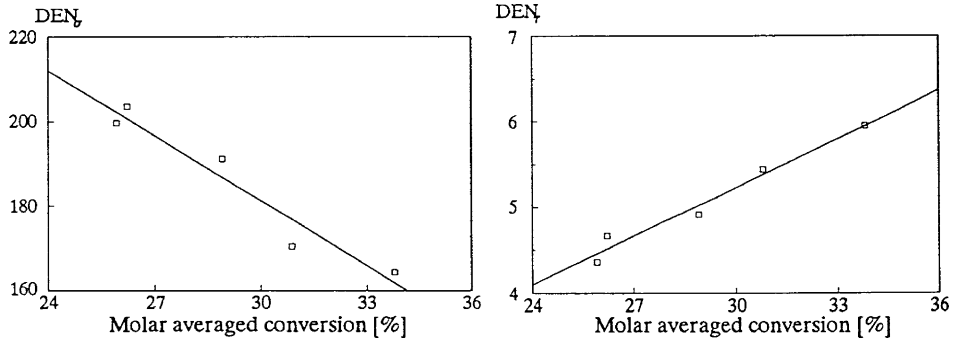

Fig. 9. HDS of LCO evolution of the denominator of the rate equations for hydrogenolysis and hydrogenation with the molar averaged conversion. Reprinted with permission from Ref. [25]. Copyright 1997, Elsevier.

Table 4
Value of the structural contributions for HDS of dibenzothiophene at 573 K

Hydrogenolysis	Hydrogenation
$K_{El,\sigma}$ and $k_{EL,\sigma}$ = 1 for all *m;n;p*	
$K_{ST,\sigma}(4;0;0)$ = 0.310	$K_{EL+ST,\tau}(m;0;0)$ = 1.04
$K_{ST,\sigma}(4;6;0)$ = 0.238	$K_{EL+ST,\tau}(m;n;0)$ = 1.11
$k_{ST,\sigma}(4;0;0)$ = 0.588	$k_{EL+ST,\tau}(m;0;0)$ = 6.05
$k_{ST,\sigma}(4;6;0)$ = 0.050	$k_{EL+ST,\tau}(m;n;0)$ = 6.07

nor on the rate coefficient of hydrogenolysis, substituents in 4- or 6-position, a fortiori in both positions, exert a strong influence on adsorption- and reaction steps in hydrogenolysis, because of steric hindrance. Me-substituted DBT have a higher rate of hydrogenation than DBT itself. The experiments with 4-MeDBT and 4,6-diMeDBT revealed that both the adsorption equilibrium constant on τ-sites and the rate coefficient were higher than those of DBT itself, for mono- as well as for di-substituted DBT [4,5]. Ma et al. related the hydrogenolysis trends with steric hindrance and the electron density of the S-atom and the hydrogenation trends with the order of the bond reacting with hydrogen [21].

In the absence of data on mono- and di-substituted model components, like 4-MeDBT and 4,6-diMeDBT, only multiplication factors f_σ and f_τ, not the structural contributions themselves, can be determined. This situation was illustrated for the benzothiophene family, (s)BT, by Vanrysselberghe and Froment [20].

With the values of the structural contributions (or multiplication factors) now available for a given catalyst, rate equations of the type (8) can be established for the conversion of (s)DBT and (s)BT in any LCO or diesel. All that is required is a relation between the rates of disappearance of one of the sDBT and the values of DEN_σ and DEN_τ that depend upon the feedstock composition and its evolution. Only a few experiments suffice for this. The products in the numerator $k_{DBT}\,K_{DBT}\,K_H$ for both σ- and τ-sites are known from the first equation of set (1) and f_{sDBT} can be calculated from the structural contributions listed in Table 4.

Finally it should be mentioned that the rate Eq. (8) of this approach can be combined with the finite rate conditioning equations in the way illustrated for thiophene removal in Section 5.

7. Reactor simulation

Commercial reactors for HDS of oil fractions operate adiabatically, with the gas phase continuous and the oil dispersed, i.e. in the trickle flow regime. Provided there is no maldistribution of the liquid this flow regime is satisfactorily described by a model assuming plug flow for both phases and transfer of heat and mass between them. The model applied here also accounts for mass transfer limitations inside the catalyst [1]. In the gas phase continuity equations for the components the transfer driving force is expressed in terms of liquid phase concentrations. C_{iG} is obtained from the Peng–Robinson equation of state and H' is a modified Henry coefficient.

(A) Continuity equations

- Gas phase

$$\frac{1}{\Omega}\frac{dF_{iG}}{dz} = -K_L a'_v\left(\frac{C_{iG}}{H'_i} - C_{iL}\right), \quad i = 1,\ldots,N,$$

$$\text{at } z = 0, \quad F_{iG} = F^0_{iG}.$$

- Liquid phase

$$\frac{1}{\Omega}\frac{dF_{iL}}{dz} = -K_l a''_v(C^s_{is} - C_{iL}) + K_L a'_v\left(\frac{C_{iG}}{H'_i} - C_{iL}\right),$$

$$\text{at } z = 0, \quad F_{iL} = F^0_{iL}.$$

- Solid phase

$$\frac{D_{ie}}{\xi^2}\frac{d}{d\xi}\left(\xi^2\frac{dC_{iS}}{d\xi}\right) = -\rho_s\sum_{j=1}^{M_I} s[j,i]r_j(C_{iS},\ldots,T_S),$$

$$\text{at } \xi = 0, \quad \frac{dC^s_{iS}}{d\xi} = 0$$

$$\text{at } \xi = \frac{d_P}{2}, \quad k_1 a''_v(C^s_{iS} - C_{iL}) = \rho_s\sum_{j=1}^{M_I}\eta_{j,i}s[j,i]r^s_j(C^s_{iS},\ldots,T_S). \tag{13}$$

Energy equations

(B) • Gas phase

$$u_{sG}\rho_G C_{pG}\frac{dT_G}{dz} = h_G a'_v(T_I - T_G) + \sum_{i=1}^{N} N_i a'_v C_{piG}(T_G - T_I),$$

$$\text{at } z = 0, \quad T_G = T^0_G.$$

- Liquid phase

$$u_{sL}\rho_L C_{pL}\frac{dT_L}{dz} = h_f a''_v(T_S - T_L) + h_L a'_v(T_I - T_L) + \sum_{i=1}^{N} N_i a'_v(\Delta H_{iv} + C_{piL}(T_I - T_L)),$$

$$\text{at } z = 0, \quad T_L = T^0_L.$$

- Solid phase

$$\rho_B\sum_{j=1}^{N_j}\eta_j r_j(C^s_{iS},\ldots,T_S)(-\Delta H_j) = h_f a''_v(T_S - T_L).$$

Pressure drop equation

(C) $$-\frac{dp_t}{dz} = (\delta_G + \delta_L)10^{[0.416/0.666+(\log_{10}(\sqrt{\delta_L/\delta_G}))^2]},$$

$$\text{at } z = 0, \quad p_t - p^0_t, \qquad \delta = f\frac{\rho u_s^2}{d_p},$$

$$f = \frac{1-\varepsilon}{\varepsilon^3}\left[1.75 + \frac{150(1-\varepsilon)}{Re}\right].$$

The pressure drop equation is that of Larkins, specific for trickle flow conditions [22]. The equation for δ is valid

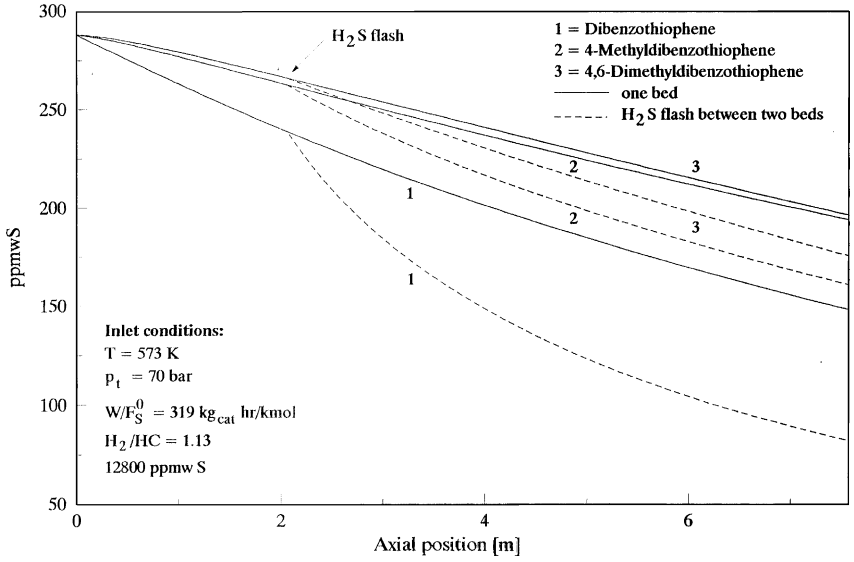

Fig. 10. HDS of diesel-type mixture. Reactor simulation. Evolution of the concentrations of DBT, 4-MeDBT and 4,6-diMeDBT along the reactor.

for both the gas and the liquid phase and for $\mathrm{Re} = d_p G/\mu(1-\varepsilon) \leq 500$. The model allows to investigate the effect of feedstock composition and operating conditions on the profiles of the concentration of the individual components, of temperature and total pressure along the reactor, but also the effect of the catalyst internal structure. It reveals for instance that, because of mass transfer limitations, in HDS of a diesel-type mixture the liquid is not saturated with hydrogen over 1/3 of a typical reactor length [1]. It also reveals that over a major fraction of the reactor substantial gradients of reacting species exist inside the catalyst particle, as shown in Table 5.

The effectiveness factors in this table are derived from the simulated internal gradients, not from an analytical solution using first order kinetics [1]. Expressed in terms of effectiveness factors it means that these are well below one, justifying more attention on the effect of the internal structure of the catalyst [23]. Deep HDS, imposed by present day and future legislation, requires serious investigation of the various aspects of HDS to reach very low S-concentrations in the reactor effluent. Fig. 10 illustrates the gain that could be expected from a two-stage reactor with an intermediate removal of H_2S, whose competitive adsorption on the σ-sites slows down the hydrogenolysis [24]. The removal restores the H_2/H_2S ratio to the feed value. The feedstock is a synthetic diesel mixture containing 110 typical components, among which 39 substituted benzothiophenes and 23 substituted dibenzothiophenes, polyaromatics and quinoline. It is mixed with a typical recycle stream mainly consisting of H_2 and H_2S. The total S-content of the liquid effluent amounts to 2124 ppmw S, instead of 2991 in the absence of intermediate H_2S removal. BT and 2,3,7-triMeDBT, e.g. are completely converted. The conversion of DBT, 4-MeDBT and 4,6-diMeDBT amounts to 73.9, 47.0 and 41.1%, instead of 52.6, 35.9 and 33.8%.

Table 5
Effectiveness factors for a number of reactions at various positions along the reactor

Reaction	Axial position (m)		
	0	1	2
DBT–BPH	0.23	0.91	0.94
DBT–CHB	0.55	0.93	0.94
DMDBT–DMBPH	0.36	0.92	0.97
DMDBT–DMCHB	0.56	0.94	0.98
BT–DHBT	0.31	0.44	–
BT–EB	0.37	0.44	–
DHBT–EB	9.9	0.63	–
Q–PB	1	1	1

DBT, dibenzothiophene; BPH, biphenyl; CHB, cydohexylbenzene; DMDBT, 4,6-dimethyldibenzothiophene; DMBPH, 4,4-dimethylbiphenyl; DMCHB, 4,6-dimethylcyclohexylbenzene; BT, benzothiophene; DHBT, dihydrobenzothiophene; EB, ethylbenzene; Q, quinoline; PB, propylbenzene.

8. Conclusion

Sufficient insight into the properties and operation of HDS catalysts has been collected to enable stepping up from the particular to the more general, from experimental data to model. Modeling of the catalyst operation in the real reactor environment is possible and the mathematical complexity is no limitation any more.What is required is a greater awareness of of the potential and the benefits of modeling and more involvement of chemical engineers in stages of development prior to the hardware design. Also required is an enhanced effort of the chemical engineering departments towards the application of fundamentals to the real problems facing the chemical industry and the profession.

Acknowledgement

B. Delmon is gratefully acknowledged for numerous stimulating discussions.

References

[1] G.F. Froment, G.A. Depauw, V. Vanrysselberghe, Ind. Eng. Chem. Res. 33 (1994) 2975.
[2] I.A. Van Parijs, G.F. Froment, lnd. Eng. Chem. Prod. Res. Dev. 25 (1986) 431–436.
[3] I.A. Van Parijs, L.H. Hosten, G.F. Froment, Ind. Eng. Chem. Prod. Res. Dev. 25 (1986) 437.
[4] V. Vanrysselberghe, G.F. Froment, Ind. Eng. Chem. Res. 35 (1996) 3311.
[5] V. Vanrysselberghe, R. Le Gall, G.F. Froment, Ind. Eng. Chem. Res. 37 (1998) 1235.
[6] G.F. Froment, B. Bischoff, Chemical Reactor Analysis and Design, 2nd ed. Wiley, New York, 1990.
[7] H. Topsoe, B.S. Clausen, F.E. Massoth, Hydrotreating Catalysis, Science and Technology, Springer-Verlag, Berlin, 1996.
[8] Y.W. Li, B. Delmon, J. Mol. Catal. A: Chem. 127 (1997) 163–190.
[9] G. Delvaux, P. Grange, B. Delmon, J. Catal. 56 (1979) 99–109.
[10] F. Bataille, J. Lemberton, P. Marchaud, G. Perot, M. Vrinat, M. Lemaire, E. Schulz, M. Breysse, S. Kasztelan, J. Catal. 191 (2000) 408–422.
[11] I.A. Van Parijs, G.F. Froment, B. Delmon, Bull. Soc. Chim. Belg. 93 (1984) 823–829.
[12] D. Pirotte, P. Grange, B. Delmon, Heterogeneous Catal. 2 (1979) 127–132.
[13] R. Candia, B.S. Clausen, H. Topsoe, J. Catal. 77 (1982) 564–566.
[14] B. Delmon, Bull. Soc. Chim. Belg. 88 (1979) 979–987.
[15] C-Y. Yu, G.F. Froment, Chem. Eng. Sci. 46 (1991) 3177–3188.
[16] M.L. Vrinat, L. de Mourgues, Appl. Catal. 5 (1983) 43–57.
[17] I.A. Van Parijs, G.F. Froment, Appl. Catal. 21 (1986) 273–285.
[18] D.H. Broderick, G.C. Schuit, G.C. Gates, J. Catal. 54 (1978) 94–97.
[19] R.C. Pille, C.Y. Yu, G.F. Froment, J. Mol. Catal. 94 (1994) 369–387.
[20] V. Vanrysselberghe, G.F. Froment, Ind. Eng. Chem. Res. 37 (1998) 4231–4240.
[21] X. Ma, K. Sakanishi, I. Mochida, Ind. Eng. Chem. Res. 35 (1996) 2487.
[22] R.P. Larkins, R.R. White, D.W. Jeffrey, AIChE J. 47 (1961) 231.
[23] L.L. Hegedus, R. Aris, A.T. Bell, M. Boudart, N.Y. Chen, H.O. Haag, G.A. Somorjai, J. Wei, Catalyst Design. Progress and Perspectives, Wiley, New York, 1987.
[24] V. Vanrysselberghe, G.F. Froment, Catalytic hydrodesulfurization. Fundamentals, kinetics, reactor simulation and process design, in: Encyclopedia of Catalysis, Wiley, New York, 2002.
[25] G.F. Froment, G.A. Depauw, V. Vanrysselberghe, Kinetics of the catalytic removal of the sulphur components from the light cycle oil of a catalytic cracking unit, in: G.F. Froment, B. Delmon, P. Grange (Eds.), Studies in Surface Science and Catalysis, vol. 106, 1997, pp. 83–97.